

# Relativistic coupled-cluster calculations for the molecular properties of $\text{AlX}^+$ (X: F, Cl, Br, I, At and Ts) ions

Ankush Thakur,<sup>1,\*</sup> Renu Bala,<sup>2,†</sup> H. S. Nataraj,<sup>1</sup> and V. S. Prasanna<sup>3,4</sup>

<sup>1</sup>*Department of Physics, Indian Institute of Technology Roorkee, Roorkee-247667, India*

<sup>2</sup>*Institute of Physics, Faculty of Physics, Astronomy and Informatics,  
Nicolaus Copernicus University, Grudziadzka 5, 87-100 Toruń, Poland*

<sup>3</sup>*Centre for Quantum Engineering, Research and Education, TCG Crest, Kolkata 700091, India*

<sup>4</sup>*Academy of Scientific and Innovative Research (AcSIR), Ghaziabad- 201002, India*

In this article, the molecular permanent electric dipole moments and components of static dipole polarizabilities for the electronic ground state of singly charged aluminum monohalides are reported. The coupled-cluster method by considering single and double excitations (CCSD) together with relativistic Dyall basis sets have been used to carry out these molecular property calculations. The contribution from triple excitations are incorporated through perturbative triples (CCSD(T)). The results from a series of progressively larger basis sets are extrapolated to the complete basis set limit. Further, the role of correlation and relativistic effects, and also the effect of augmentation over the considered basis sets on the valence molecular properties are studied. Our results are compared with those available in the literature.

**Keywords:** coupled-cluster, electric dipole moment, static dipole polarizability.

## I. INTRODUCTION

The study of ultracold diatomic molecules has garnered significant interest in recent decades owing to their wide range of potential applications [1–4], including fundamental physics [5], quantum chemistry [6], quantum simulation [7], etc. An important molecular property that holds significance in many of these applications is the permanent electric dipole moment (PDM) of a molecule. PDMs are important for the study of dipole-dipole interactions [1, 8], quantum computing [9–11], quantum information theory [12], and they are useful for exploring the characteristics of intermolecular forces [13]. PDMs play a crucial role in molecular experiments aimed at detecting the electron electric dipole moment [14], serving as a probe for new physics beyond the standard model of elementary particles [15–18]. The importance of PDM lies in its contribution to understanding the chaining of molecules confined in a 1D optical lattice, where the interaction strength in the process of molecular chaining is directly related to the PDM. [19].

The static electric dipole polarizability (DP) of molecules is another important property with key

applications in ultracold physics. Electric DP plays a significant role in linear and non-linear optical phenomena [20], electron-molecule interactions [21], and also provides valuable information for studies on molecular collision processes [22]. Both PDM and electric DP are crucial for determining the infrared and Raman molecular spectra [23]. Therefore, these properties are crucial in understanding the physics of ultracold molecules.

In the present work, we have studied the PDMs and the static electric DPs of aluminum monohalide ( $\text{AlX}^+$  where  $X = \text{F, Cl, Br, I, At}$  and  $\text{Ts}$ ) systems. These findings could be relevant for various future applications, considering the recent focus on laser cooling of molecular ions, and theoretical studies indicating the potential for laser cooling of  $\text{AlF}^+$  and  $\text{AlCl}^+$  molecular ions [24]. A few theoretical studies have been conducted on aluminum monohalide systems, in which their PDMs were reported. Klein and Rosmus [25] have calculated the PDM for  $\text{AlF}^+$  molecule using the pseudo-natural orbital configuration interaction (PNO CI) method with coupled electron pair approximation (CEPA). The study of PDM for  $\text{AlF}^+$  and  $\text{AlCl}^+$  molecular ions have been reported by Glenwinkel-Meyer *et al* [26] using multi-reference configuration interaction (MRCI) method. Recently, Kang *et al* [24] employed the MRCI method with Davidson correction (MRCI+Q) to calculate the PDM of  $\text{AlCl}^+$  molecular ion. Quite recently, the PDMs of  $\text{AlX}^+$  ions have been studied by Bala *et al* [27] using Kramers-restricted configuration interaction method

\* ankush\_t@ph.iitr.ac.in; Contributed equally to the work

† balar180@gmail.com; Contributed equally to the work

considering single and double excitations (KRCISD). However, to the best of our knowledge, there is no work in literature that reports the static electric DPs of these systems.

In our work, the relativistic calculations for the molecular properties have been performed using CCSD method over the Dirac-Hartree-Fock (DHF) reference state. Additionally, we have reported the molecular properties at the CCSD(T) level of theory. To carry out these calculations, we have used relativistic Dyal basis sets of double, triple and quadruple zeta quality [28, 29]. Using these hierarchy of basis sets, we have extrapolated these properties to the complete basis set limit. The reported results show good agreement with the existing values of the dipole moments. We have studied the impact of electron correlation effects and relativistic effects on the molecular properties considered in this work.

This paper is divided into four sections. After the introduction in Section I, the theory and calculation details are given in Section II. A detailed discussion of the computed results is presented in Section III. The section IV summarizes the current work.

## II. THEORY AND METHODOLOGY

### A. Theory

The correlated wavefunction ( $|\Psi_{CC}\rangle$ ) in the coupled-cluster (CC) method is expressed as the exponential of the cluster operator  $\hat{T}$  acting on the DHF wavefunction ( $|\Phi_0\rangle$ ) [30]:

$$|\Psi_{CC}\rangle = e^{\hat{T}}|\Phi_0\rangle \quad (1)$$

Expanding the exponential operator  $e^{\hat{T}}$  into a series yields:

$$|\Psi_{CC}\rangle = \left[ 1 + \hat{T}_1 + \frac{1}{2}\hat{T}_1^2 + \hat{T}_2 + \frac{1}{3!}\hat{T}_1^3 + \hat{T}_1\hat{T}_2 + \hat{T}_3 \dots \right] |\Phi_0\rangle \quad (2)$$

where  $\hat{T}$  ( $= \hat{T}_1 + \hat{T}_2 + \hat{T}_3 \dots + \hat{T}_n$ , for an n-electron system) is the cluster operator;  $\hat{T}_1, \hat{T}_2, \hat{T}_3, \dots, \hat{T}_n$  correspond to operators that enumerate all possible single excitations, double excitations, triple excitations,  $\dots$ , n-tuple excitations that arise from the reference DHF state. In second quantized notation, these operators can be expressed as,

$$\hat{T}_1 = \sum_{a,p} t_a^p \hat{a}_p^\dagger \hat{a}_a, \quad (3)$$

$$\hat{T}_2 = \frac{1}{4} \sum_{ab,pq} t_{ab}^{pq} \hat{a}_p^\dagger \hat{a}_q^\dagger \hat{a}_b \hat{a}_a, \quad (4)$$

and so on, where the subscripts  $a, b, c, \dots$  represent filled spin-orbitals, and  $p, q, r, \dots$  denote the virtual spin-orbitals. Thus, the operator  $\hat{T}_1$  denotes the annihilation of an electron from the filled spin-orbital  $a$ , accompanied by the creation of a virtual electron in spin-orbital  $p$ , and this single excitation is weighted by the amplitude  $t_a^p$ . Similarly,  $\hat{T}_2$  signifies the simultaneous annihilation of a pair of electrons from the filled spin-orbitals ( $a, b$ ) and their creation in the virtual spin-orbitals ( $p, q$ ), with an associated amplitude,  $t_{ab}^{pq}$ .

We employ the finite-field method to compute molecular properties. In the presence of a uniform external electric field of strength  $\epsilon$ , the total energy  $E(\epsilon)$  of a molecule can be expressed as a Taylor series expansion [31]:

$$E(\epsilon) = E_0 - \mu\epsilon - \frac{1}{2}\alpha\epsilon^2 + \dots, \quad (5)$$

where

$$\mu = -\frac{dE(\epsilon)}{d\epsilon}; \quad \alpha = -\frac{d^2E(\epsilon)}{d\epsilon^2}. \quad (6)$$

where  $\mu$  is the PDM and  $\alpha$  is the static DP.

### B. Details of calculation

The PDM and the static electric DP ( $\alpha_{\parallel}$  and  $\alpha_{\perp}$ ) calculations reported in this work are computed at different levels of theory using DIRAC23 [32] software package. We utilize a 4-component wavefunction, which is expanded using distinct basis sets for both large and small components. The kinetic balance condition is applied to smaller components to prevent the wavefunction from experiencing a variational collapse into the negative energy continuum [33]. The DHF Coulomb Hamiltonian is employed with the approximation proposed by Visscher [34], wherein the contribution from the (SS|SS) integrals is replaced by an inter-atomic correction. We have used the uncontracted Dyal basis sets for the calculations. The details of the basis functions are shown in Table I. The values of equilibrium bond lengths used in this

work are [27]: 1.623 Å for  $\text{AlF}^+$ , 2.058 Å for  $\text{AlCl}^+$ , 2.223 Å for  $\text{AlBr}^+$ , 2.512 Å for  $\text{AlI}^+$ , 2.768 Å for  $\text{AlAt}^+$ , and 2.928 Å for  $\text{AlTs}^+$ . The strength of the electric field taken as perturbation is chosen in the range of  $-1 \times 10^{-4}$  to  $1 \times 10^{-4}$  au. The aluminum atom is chosen to be at the origin of the coordinate axes.

Table I. Details of the basis functions.

Atom	Basis	Basis functions
Al	dyall.v2z	12s, 8p, 1d
	dyall.v3z	18s, 11p, 2d, 1f
	dyall.v4z	24s, 14p, 3d, 2f, 1g
	s-aug-dyall.v4z	25s, 15p, 4d, 3f, 2g
F	dyall.v2z	10s, 6p, 1d
	dyall.v3z	14s, 8p, 2d, 1f
	dyall.v4z	18s, 10p, 3d, 2f, 1g
	s-aug-dyall.v4z	19s, 11p, 4d, 3f, 2g
Cl	dyall.v2z	12s, 8p, 1d
	dyall.v3z	18s, 11p, 2d, 1f
	dyall.v4z	24s, 14p, 3d, 2f, 1g
	s-aug-dyall.v4z	25s, 15p, 4d, 3f, 2g
Br	dyall.v2z	15s, 11p, 7d
	dyall.v3z	23s, 16p, 10d, 1f
	dyall.v4z	30s, 21p, 13d, 2f, 1g
	s-aug-dyall.v4z	31s, 22p, 14d, 3f, 2g
I	dyall.v2z	21s, 15p, 11d
	dyall.v3z	28s, 21p, 15d, 1f
	dyall.v4z	33s, 27p, 18d, 2f, 1g
	s-aug-dyall.v4z	34s, 28p, 19d, 3f, 2g
At	dyall.v2z	24s, 20p, 14d, 8f
	dyall.v3z	30s, 26p, 17d, 11f
	dyall.v4z	34s, 31p, 21d, 14f, 1g
	s-aug-dyall.v4z	35s, 32p, 22d, 15f, 2g
Ts	dyall.v2z	26s, 23p, 17d, 10f
	dyall.v3z	30s, 29p, 20d, 13f
	dyall.v4z	35s, 35p, 24d, 16f, 1g
	s-aug-dyall.v4z	36s, 36p, 25d, 17f, 2g

By considering the z-axis as the internuclear axis of the molecule, we obtain two components of DP: one along ( $\alpha_{\parallel} \equiv \alpha_{zz}$ ) and the other perpendicular ( $\alpha_{\perp} \equiv \alpha_{xx} \equiv \alpha_{yy}$ ) to the direction of internuclear axis. The average and the anisotropic polarizabilities, ( $\bar{\alpha}$ ) and ( $\gamma$ ) respectively, are given by,

$$\bar{\alpha} = (\alpha_{\parallel} + 2\alpha_{\perp})/3 \quad (7)$$

$$\gamma = \alpha_{\parallel} - \alpha_{\perp}. \quad (8)$$

The cutoff energy of  $12E_h$  is consistently set for all molecules to limit the higher virtual orbitals, thereby re-

ducing computational expenses. The details of the active electrons and virtual orbitals for different basis sets are shown in Table II.

Table II. Details of the number of active electrons and virtual orbitals for  $\text{AlX}^+$  (X: F, Cl, Br, I, At and Ts) molecular systems in different basis sets.

Molecule	Active electrons	Basis	Virtual orbitals
$\text{AlF}^+$	15	dyall.v2z	35
		dyall.v3z	63
		dyall.v4z	102
		s-aug-dyall.v4z	143
$\text{AlCl}^+$	15	dyall.v2z	32
		dyall.v3z	64
		dyall.v4z	115
		s-aug-dyall.v4z	165
$\text{AlBr}^+$	25	dyall.v2z	37
		dyall.v3z	69
		dyall.v4z	120
		s-aug-dyall.v4z	170
$\text{AlI}^+$	25	dyall.v2z	42
		dyall.v3z	74
		dyall.v4z	125
		s-aug-dyall.v4z	170
$\text{AlAt}^+$	29	dyall.v2z	49
		dyall.v3z	85
		dyall.v4z	138
		s-aug-dyall.v4z	188
$\text{AlTs}^+$	29	dyall.v2z	56
		dyall.v3z	84
		dyall.v4z	137
		s-aug-dyall.v4z	187

The results calculated systematically using three progressively larger basis sets, are extrapolated to the complete basis set CBS limit using a function of the form [35]:

$$f(x) = f_{CBS} + Be^{-(x-1)} + Ce^{-(x-1)^2} \quad (9)$$

where  $B$  and  $C$  are constant parameters,  $x = 2, 3, 4$  is the cardinal number for double, triple and quadruple zeta basis sets respectively,  $f(x)$  represents the value of the property calculated with the basis set characterized by the cardinal number  $x$ , and  $f_{CBS}$  denotes the value of the property of interest at the CBS limit. This approach for computing the CBS limit for molecular properties has been applied in the literature [36, 37].

### III. RESULTS AND DISCUSSION

The computed results for the molecular properties are discussed in the upcoming subsections. We also investi-

gate the relative percentage difference in the values of PDM and DP for the  $\text{AlX}^+$  molecular systems due to electron correlation and relativistic effects. For the relative percentage change due to correlation effects, we define  $\delta_P^{\text{corr}}$  as:

$$\delta_P^{\text{corr}} = \left( \frac{P_{\text{CCSD(T)}} - P_{\text{DHF}}}{P_{\text{DHF}}} \times 100 \right) \% \quad (10)$$

This indicates the relative percentage of correlation effects contributing to the property  $P$ .

For the relative percentage change due to relativistic effects, we define  $\delta_P^{\text{rel}}$  as:

$$\delta_P^{\text{rel}} = \left( \frac{P_{\text{Rel}} - P_{\text{Non-Rel}}}{P_{\text{Non-Rel}}} \times 100 \right) \% \quad (11)$$

All the reported values for the molecular properties have been rounded off to three decimal places in this work. Our final results at the CBS limit are shown in bold font in Table III and Table IV.

### A. Permanent electric dipole moments

Table III shows the results for the magnitude of the PDMs of singly charged aluminum monohalides calculated in the present work, compared with the results available in the literature. The PDM is negative for  $\text{AlF}^+$  and  $\text{AlCl}^+$ , whereas it is positive for the remaining molecules, and it increases as one progresses from lighter to heavier systems, as shown in Figure 1. As molecules become heavier, the PDM tends to increase due to their larger atomic size, resulting in stronger charge separation.

For all the molecular ions, the PDM values at the DHF level show good agreement with those available in the literature [25, 27]. For the  $\text{AlF}^+$  molecule, the dipole moment value at the CCSD(T) level compares well, differing by approximately 4.9% from that at the KRCISD level, as reported in Ref. [27], all under a similar standard of basis set and equilibrium bond length but with different active spaces.

Glenewinkel-Meyer *et al* [26] calculated the PDM of the  $\text{AlF}^+$  molecule using complete active space self-consistent-field (CASSCF) and internally contracted MRCI methods. They employed Gaussian-type orbital basis sets, including Partridge's  $17s$ ,  $12p$  for Al and Dunning's quadruple zeta for F. Subsequent MRCI calculations, included in their work, comprised all

Table III. Magnitude of permanent electric dipole moments (in Debye) for  $\text{AlX}^+$  (X: F, Cl, Br, I, At and Ts) molecular systems at different levels of correlation and basis sets.

Molecule	Basis	Method	$\mu$	Ref.	
$\text{AlF}^+$	dyall.v2z	DHF	2.821	This work	
		CCSD	2.436	This work	
		CCSD(T)	2.327	This work	
	dyall.v3z	DHF	2.569	This work	
		CCSD	2.296	This work	
		CCSD(T)	2.210	This work	
	dyall.v4z	DHF	2.550	This work	
		CCSD	2.300	This work	
		CCSD(T)	2.220	This work	
	<b>CBS</b>	DHF	DHF	2.546	This work
			CCSD	2.308	This work
			<b>CCSD(T)</b>	<b>2.231</b>	This work
		KRCISD	DHF	2.56	[27]
			KRCISD	2.33	[27]
			MRCI	2.40	[26]
HF			2.39	[25]	
PNO-CEPA	2.29	[25]			
$\text{AlCl}^+$	dyall.v2z	DHF	0.937	This work	
		CCSD	0.279	This work	
		CCSD(T)	0.121	This work	
	dyall.v3z	DHF	0.768	This work	
		CCSD	0.293	This work	
		CCSD(T)	0.155	This work	
	dyall.v4z	DHF	0.746	This work	
		CCSD	0.346	This work	
		CCSD(T)	0.217	This work	
	<b>CBS</b>	DHF	DHF	0.737	This work
			CCSD	0.381	This work
			<b>CCSD(T)</b>	<b>0.258</b>	This work
		KRCISD	DHF	0.76	[27]
			KRCISD	0.47	[27]
			MRCI	0.27	[24]
MRCI			0.19	[26]	
$\text{AlBr}^+$	dyall.v2z	DHF	0.663	This work	
		CCSD	0.129	This work	
		CCSD(T)	0.307	This work	
	dyall.v3z	DHF	0.493	This work	
		CCSD	0.126	This work	
		CCSD(T)	0.285	This work	
	dyall.v4z	DHF	0.486	This work	
		CCSD	0.038	This work	
		CCSD(T)	0.192	This work	
	<b>CBS</b>	DHF	DHF	0.487	This work
			CCSD	0.021	This work
			<b>CCSD(T)</b>	<b>0.130</b>	This work

Table III. Continued...

		DHF	0.50	[27]
		KRCISD	0.07	[27]
AlI <sup>+</sup>	dyall.v2z	DHF	1.269	This work
		CCSD	2.434	This work
		CCSD(T)	2.636	This work
	dyall.v3z	DHF	1.493	This work
		CCSD	2.472	This work
		CCSD(T)	2.654	This work
	dyall.v4z	DHF	1.501	This work
		CCSD	2.342	This work
		CCSD(T)	2.524	This work
	<b>CBS</b>	DHF	1.499	This work
		CCSD	2.253	This work
		<b>CCSD(T)</b>	<b>2.435</b>	This work
		DHF	1.49	[27]
		KRCISD	2.16	[27]
AlAt <sup>+</sup>	dyall.v2z	DHF	4.033	This work
		CCSD	4.281	This work
		CCSD(T)	4.357	This work
	dyall.v3z	DHF	4.292	This work
		CCSD	4.396	This work
		CCSD(T)	4.428	This work
	dyall.v4z	DHF	4.304	This work
		CCSD	4.299	This work
		CCSD(T)	4.316	This work
	<b>CBS</b>	DHF	4.303	This work
		CCSD	4.229	This work
		<b>CCSD(T)</b>	<b>4.238</b>	This work
		DHF	4.31	[27]
		KRCISD	4.24	[27]
AlTs <sup>+</sup>	dyall.v2z	DHF	6.444	This work
		CCSD	6.623	This work
		CCSD(T)	6.802	This work
	dyall.v3z	DHF	6.696	This work
		CCSD	6.687	This work
		CCSD(T)	6.826	This work
	dyall.v4z	DHF	6.722	This work
		CCSD	6.581	This work
		CCSD(T)	6.697	This work
	<b>CBS</b>	DHF	6.731	This work
		CCSD	6.507	This work
		<b>CCSD(T)</b>	<b>6.609</b>	This work
		DHF	6.76	[27]
		KRCISD	6.91	[27]

single and double excitations relative to the CASSCF reference functions, incorporating correlations for all valence electrons. They obtain a PDM of 2.40 Debye (D), indicating a 0.17 D increase compared to our result of 2.231 (D) (at CCSD(T) level). In addition to the difference in the methods, their basis set size and selection of active space are considerably smaller in comparison to ours.

Klein and Rosmus [25] have reported the PDM for AlF<sup>+</sup> molecule. They employed PNO CI method with CEPA approximation, utilizing a GTO basis set with 12s, 9p, and 2d functions for Al, and 10s, 6p, and 2d functions for F. Within the CI level, they considered single and double excitations relative to the reference HF state. To assess the impact of excitations higher than single and double levels, they employed the CEPA approximation in their work. In our work, the value of PDM at the CCSD(T) level exceeds that reported in their study at the PNO-CEPA level by 2.6%. This difference could be due to the different methods and large basis set employed in our work.

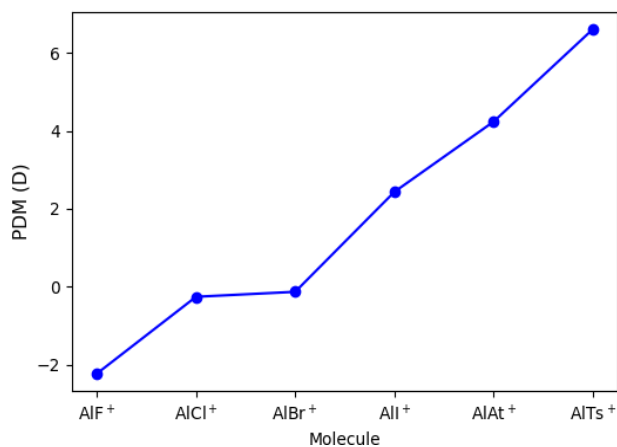


Figure 1. The CBS values for molecular PDMs for the ground state of AlX<sup>+</sup> (X: F, Cl, Br, I, At and Ts) molecular systems at CCSD(T) level of theory.

For the AlCl<sup>+</sup> molecule, the value of PDM reported in our work using the CCSD(T) method is 0.012 D smaller and 0.068 D larger than those reported in Ref. [24] and Ref. [26], respectively, at MRCI level of theory. Our value of PDM at the CCSD(T) level is smaller by 0.212 D compared to that reported in Ref. [27] at the KRCISD level.

Bala *et al* [27] had computed the PDM of AlBr<sup>+</sup>, AlI<sup>+</sup>,

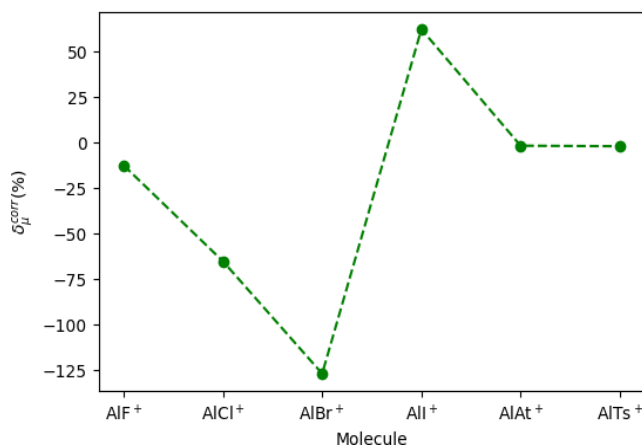


Figure 2. Figure showing the relative percentage changes in the values of PDMs in the  $\text{AlX}^+$  (X: F, Cl, Br, I, At and Ts) molecular systems due to the electron correlation effects.

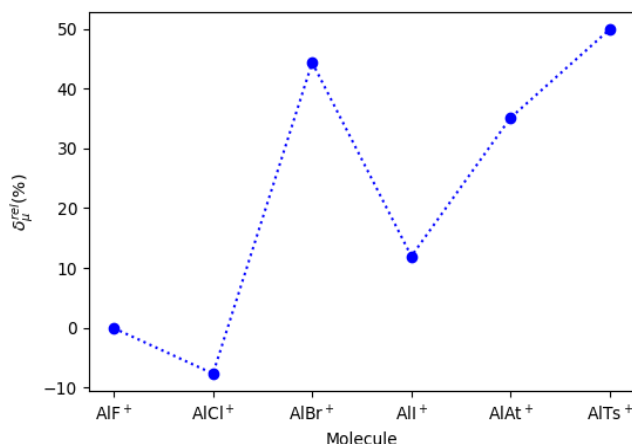


Figure 3. Figure showing the relative percentage changes in the values of PDMs in the  $\text{AlX}^+$  (X: F, Cl, Br, I, At and Ts) molecular systems due to the relativistic effects.

AlAt<sup>+</sup>, and AlTs<sup>+</sup> molecules at the DHF and KRCISD levels of theory using dyall.v4z basis sets. Our results show good agreement with those reported in their work. Our PDM values at CCSD(T) levels show increments of 0.06 D, 0.275 D, 0.002 D, and 0.301 D for AlBr<sup>+</sup>, AlI<sup>+</sup>, AlAt<sup>+</sup>, and AlTs<sup>+</sup>, respectively, in comparison to those reported by them at KRCISD level. These differences in the results could be due to the ability of CC to capture more electron correlation effects than CI [38, 39].

Electron correlation significantly affects the accuracy of final values, with its impact reaching maximum in the CCSD(T) calculations for AlI<sup>+</sup>, where the correlation fraction (denoted as  $\delta_{\mu}^{\text{corr}}$  in Figure 2) constitutes approximately 62%. For AlF<sup>+</sup> and AlCl<sup>+</sup> molecular ions, the values of PDM decrease from the DHF method to the CCSD(T) method, whereas AlI<sup>+</sup> exhibits a contrasting trend with an increase in value. The PDM value of the AlBr<sup>+</sup>, AlAt<sup>+</sup>, and AlTs<sup>+</sup> molecular ions decreases from the DHF to the CCSD method, followed by an increase in the CCSD(T) method. In summary, electron correlation effects leads to an increase in the PDM value for AlI<sup>+</sup> molecular ion, whereas it results in a decrease in the PDM value for the remaining molecular ions. Figure 2 illustrates these observed trends.

We now compare the PDM results obtained from both non-relativistic and relativistic methods, using the data presented in Table V. The HF Coulomb Hamiltonian has been employed for non-relativistic calculations. In Figure 3, we have depicted the fractional percentage difference in PDM values due to relativistic effects (denoted as  $\delta_{\mu}^{\text{rel}}$ ). The effect of relativity seems to decrease the value of PDM for lighter molecular ions, such as AlF<sup>+</sup> and AlCl<sup>+</sup>, and to increase the value for other molecular ions. We observe that the significance of relativistic effects is most notable in the heavier molecules, naturally as anticipated, with the PDM of AlAt<sup>+</sup> and AlTs<sup>+</sup> molecular ions showing the change of 35% and 50%, respectively, with the inclusion of relativistic effects.

As the molecular properties studied in this work are valence properties, the addition of diffuse functions to the basis sets can play an important role in the accuracy of results [40]. Therefore, we have also studied the effect of augmentation of basis sets on the results of PDM by considering singly augmented quadruple zeta basis sets, as shown in Table VI. The difference in our final results of PDMs between the un-augmented and augmented basis sets is about 0.001 D for AlF<sup>+</sup>, 0.005 D for AlCl<sup>+</sup>, 0.007 D for AlBr<sup>+</sup>, 0.012 D for AlI<sup>+</sup>, 0.007 D for AlAt<sup>+</sup>, and 0.01 D for AlTs<sup>+</sup> at the CCSD(T) level. Thus, the augmentation of the basis sets does not alter the results of the PDMs by more than 3.6%.

In order to understand the errors in our calculation, we have considered the heavy AlAt<sup>+</sup> molecule as our representative system. One potential source of uncertainty in our calculation may stem from the exclusion of

more number of active electrons. To address this point, we have incorporated 49 active electrons rather than 29 in our active space. This results in a 1.7% change in the value of PDM. We have found a 1.9% change in the PDM due to the increase in the virtual cut-off from 12  $E_h$  to 25  $E_h$  and a 1.7% change with the addition of augmented functions to the basis sets. We now consider the error resulting from the missing triple excitations in the CCSD(T) method. This method is widely recognized as the gold standard for molecular property calculations [41], and we anticipate that the error due to missing triple excitations would be significantly lower than the percentage difference between the CCSD and CCSD(T) values, which we found to be 0.2%. All these variations result in a total change of about 5.5% in the PDM value.

### B. Static electric dipole polarizabilities

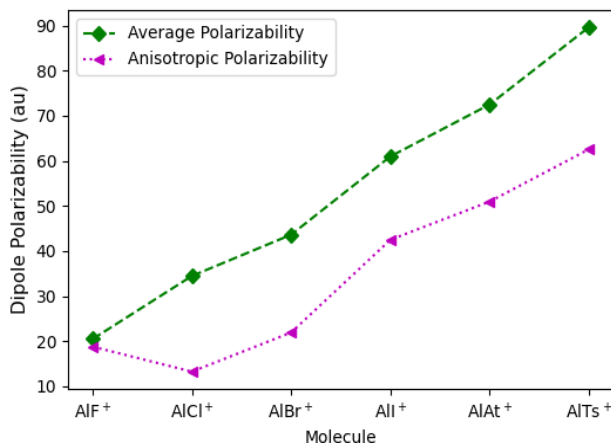


Figure 4. The CBS values for the average and anisotropic component of polarizability for the ground state of  $\text{AlX}^+$  (X: F, Cl, Br, I, At and Ts) molecular systems at CCSD(T) level of theory.

The computed results for the components of static DP are collected in Table IV. The results of electric DPs for these molecular ions are not available in the literature, to the best of our knowledge, for comparison. We prioritize analyzing the trends of  $\bar{\alpha}$  and  $\gamma$  as they are experimentally measurable [42]. Figure 4 shows the variation of CBS values of average and anisotropic components of DP for all the molecules at the CCSD(T) level of theory. The average polarizability increases from  $\text{AlF}^+$  to  $\text{AlTs}^+$ , and the anisotropic polarizability

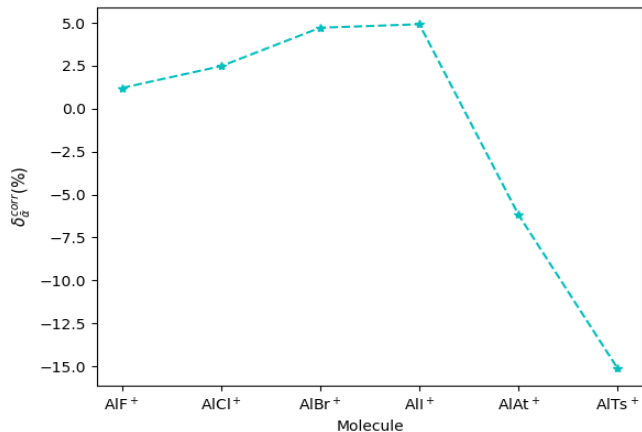


Figure 5. Figure showing the relative percentage changes in the  $\bar{\alpha}$  values of the  $\text{AlX}^+$  (X: F, Cl, Br, I, At and Ts) molecular systems due to the electron correlation effects.

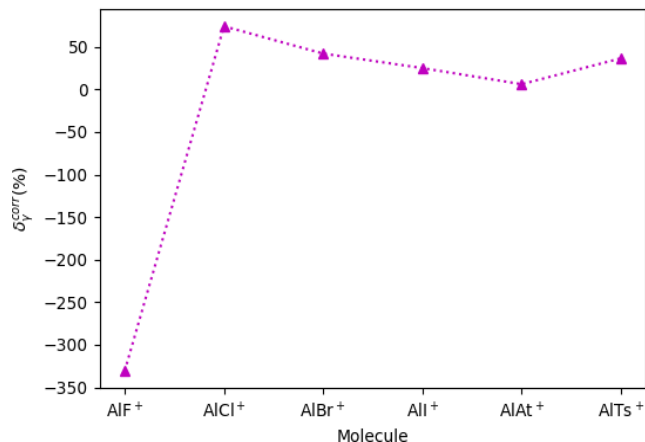


Figure 6. Figure showing the relative percentage changes in the  $\gamma$  values of the  $\text{AlX}^+$  (X: F, Cl, Br, I, At and Ts) molecular systems due to the electron correlation effects.

follows the same trend, except for  $\text{AlCl}^+$ .

We start by discussing the correlation effects, based on Figures 5 and 6, which show the fractional percentage difference in the values of  $\bar{\alpha}$  (denoted as  $\delta_{\bar{\alpha}}^{\text{corr}}$ ) and  $\gamma$  (denoted as  $\delta_{\gamma}^{\text{corr}}$ ), respectively, due to correlation effects. Electron correlation effects cause a decrease in the  $\bar{\alpha}$  value for heavier molecular ions like  $\text{AlAt}^+$  and  $\text{AlTs}^+$ , while resulting in an increase in the  $\bar{\alpha}$  value for

Table IV. Components of static dipole polarizability (in au) for  $AlX^+$  ( $X$ : F, Cl, Br, I, At and Ts) molecular systems at different levels of correlation, computed in this work.

Molecule	Basis	Method	$\alpha_{\parallel}$	$\alpha_{\perp}$	$\bar{\alpha}$	$\gamma$	
$AlF^+$	dyall.v2z	DHF	16.256	20.240	18.912	-3.984	
		CCSD	18.889	20.427	19.914	-1.538	
		CCSD(T)	19.680	20.512	20.235	-0.832	
	dyall.v3z	DHF	16.723	21.300	19.774	-4.577	
		CCSD	18.981	21.393	20.589	-2.412	
		CCSD(T)	19.654	21.485	20.875	-1.831	
	dyall.v4z	DHF	16.857	21.678	20.071	-4.821	
		CCSD	19.080	21.637	20.785	-2.557	
		CCSD(T)	27.610	17.180	20.657	10.430	
	<b>CBS</b>	DHF	-	-	20.242	-4.965	
		CCSD	-	-	20.894	-2.625	
		<b>CCSD(T)</b>	-	-	<b>20.487</b>	<b>18.763</b>	
	$AlCl^+$	dyall.v2z	DHF	36.275	26.144	29.521	10.131
			CCSD	41.563	26.572	31.569	14.991
			CCSD(T)	42.800	26.689	32.059	16.111
dyall.v3z		DHF	38.234	29.406	32.349	8.828	
		CCSD	43.007	29.636	34.093	13.371	
		CCSD(T)	44.254	29.756	34.589	14.498	
dyall.v4z		DHF	38.549	30.480	33.170	8.069	
		CCSD	42.996	30.551	34.699	12.445	
		CCSD(T)	43.706	29.996	34.566	13.710	
<b>CBS</b>		DHF	-	-	33.627	7.601	
		CCSD	-	-	35.021	11.875	
		<b>CCSD(T)</b>	-	-	<b>34.462</b>	<b>13.233</b>	
$AlBr^+$		dyall.v2z	DHF	48.506	29.701	35.969	18.805
			CCSD	54.899	30.235	38.456	24.664
			CCSD(T)	56.194	30.361	38.972	25.833
	dyall.v3z	DHF	51.314	34.368	40.017	16.946	
		CCSD	57.271	34.662	42.198	22.609	
		CCSD(T)	58.569	34.806	42.727	23.763	
	dyall.v4z	DHF	51.742	35.732	41.069	16.010	
		CCSD	57.289	35.820	42.976	21.469	
		CCSD(T)	58.411	35.788	43.329	22.623	
	<b>CBS</b>	DHF	-	-	41.640	15.441	
		CCSD	-	-	43.372	20.769	
		<b>CCSD(T)</b>	-	-	<b>43.606</b>	<b>21.924</b>	

the remaining molecular ions. These effects lead to an increase in the  $\gamma$  value for all molecular ions, with  $AlCl^+$  showing the highest fractional percentage difference between CCSD(T) and DHF results, approximately 74%.

Figure 6 shows a significantly different value of  $\delta_{\gamma}^{corr}$  for  $AlF^+$  molecular ion compared to the other molecular ions. This discrepancy is due to the large difference in



Table IV. Continued...

AlI <sup>+</sup>	dyall.v2z	DHF	77.196	37.036	50.423	40.160	
		CCSD	86.241	38.072	54.128	48.169	
		CCSD(T)	87.056	38.173	54.467	48.883	
	dyall.v3z	DHF	79.804	44.019	55.947	35.785	
		CCSD	88.256	44.432	59.040	43.824	
		CCSD(T)	88.978	44.546	59.357	44.432	
	dyall.v4z	DHF	80.426	45.804	57.345	34.622	
		CCSD	88.449	45.835	60.040	42.614	
		CCSD(T)	89.195	46.023	60.414	43.172	
	<b>CBS</b>	DHF	-	-	58.099	33.988	
		CCSD	-	-	60.546	41.947	
		<b>CCSD(T)</b>	-	-	<b>60.959</b>	<b>42.474</b>	
	AlAt <sup>+</sup>	dyall.v2z	DHF	103.810	57.430	72.890	46.380
			CCSD	100.210	58.220	72.217	41.990
			CCSD(T)	102.700	50.580	67.953	52.120
dyall.v3z		DHF	107.860	59.279	75.473	48.581	
		CCSD	102.620	57.900	72.807	44.720	
		CCSD(T)	104.960	53.210	70.460	51.750	
dyall.v4z		DHF	108.780	60.480	76.580	48.300	
		CCSD	103.230	58.690	73.537	44.540	
		CCSD(T)	105.880	54.620	71.707	51.260	
<b>CBS</b>		DHF	-	-	77.239	48.033	
		CCSD	-	-	74.010	44.323	
		<b>CCSD(T)</b>	-	-	<b>72.464</b>	<b>50.941</b>	
AlTs <sup>+</sup>		dyall.v2z	DHF	133.630	87.051	102.577	46.579
			CCSD	132.190	60.520	84.410	71.670
			CCSD(T)	133.859	3.810	47.160	130.049
	dyall.v3z	DHF	134.811	89.620	104.684	45.191	
		CCSD	132.061	58.529	83.040	73.532	
		CCSD(T)	133.520	31.930	65.793	101.590	
	dyall.v4z	DHF	135.630	90.080	105.263	45.550	
		CCSD	131.010	58.663	82.779	72.347	
		CCSD(T)	132.180	54.477	80.378	77.703	
	<b>CBS</b>	DHF	-	-	105.581	45.841	
		CCSD	-	-	82.650	71.480	
		<b>CCSD(T)</b>	-	-	<b>89.599</b>	<b>62.530</b>	

the value of  $\gamma$  at the DHF and CCSD(T) levels of theory. We have discussed the reason for the discrepancy in values in the later part of the manuscript.

After discussing the correlation effects, we now address the effects of relativity on the components of static

DP. We compare the relativistic and non-relativistic results of  $\bar{\alpha}$  and  $\gamma$  for all the molecules, as shown in Table V. Additionally, the fractional percentage difference in the values of  $\bar{\alpha}$  (denoted as  $\delta_{\bar{\alpha}}^{\text{rel}}$ ) and  $\gamma$  (denoted as  $\delta_{\gamma}^{\text{rel}}$ ) due to relativistic effects is plotted in Figures 7 and 8, respectively. The relativistic effects decrease the value of

Table V. Comparison of the magnitudes of PDMs (in Debye) and components of static dipole polarizability (in au) obtained from relativistic and non-relativistic calculations at different levels of correlation using dyall.v4z basis sets.

Molecule	Method	Non-relativistic			Relativistic		
		$\mu$	$\bar{\alpha}$	$\gamma$	$\mu$	$\bar{\alpha}$	$\gamma$
AlF <sup>+</sup>	HF/DHF	2.547	20.153	-4.957	2.550	20.071	-4.821
	CCSD	2.301	20.851	-2.886	2.300	20.785	-2.557
	CCSD(T)	2.221	10.723	13.275	2.220	20.657	10.430
AlCl <sup>+</sup>	HF/DHF	0.757	33.187	7.828	0.746	33.170	8.069
	CCSD	0.363	35.053	12.270	0.346	34.699	12.445
	CCSD(T)	0.235	34.201	15.372	0.217	34.566	13.710
AlBr <sup>+</sup>	HF/DHF	0.531	40.994	15.457	0.486	41.069	16.010
	CCSD	0.022	43.055	21.965	0.038	42.976	21.469
	CCSD(T)	0.133	43.489	23.337	0.192	43.329	22.623
AlI <sup>+</sup>	HF/DHF	1.295	56.356	31.709	1.501	57.345	34.622
	CCSD	2.056	58.247	36.354	2.342	60.040	42.614
	CCSD(T)	2.254	58.785	37.402	2.524	60.414	43.172
AlAt <sup>+</sup>	HF/DHF	2.053	70.403	52.420	4.304	76.580	48.300
	CCSD	3.036	72.870	57.960	4.299	73.537	44.540
	CCSD(T)	3.194	72.623	56.140	4.316	71.707	51.260
AlTs <sup>+</sup>	HF/DHF	3.380	85.077	67.970	6.722	105.263	45.550
	CCSD	4.326	81.350	56.669	6.581	82.779	72.347
	CCSD(T)	4.467	77.017	60.829	6.697	80.378	77.703

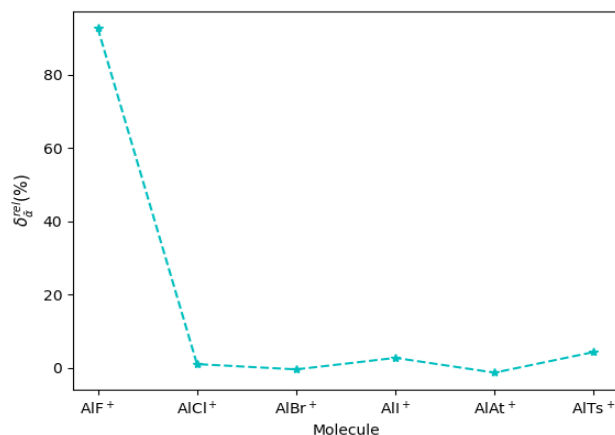


Figure 7. Figure showing the relative percentage changes in the  $\bar{\alpha}$  values of the AlX<sup>+</sup> (X: F, Cl, Br, I, At and Ts) molecular systems due to the electron relativistic effects.

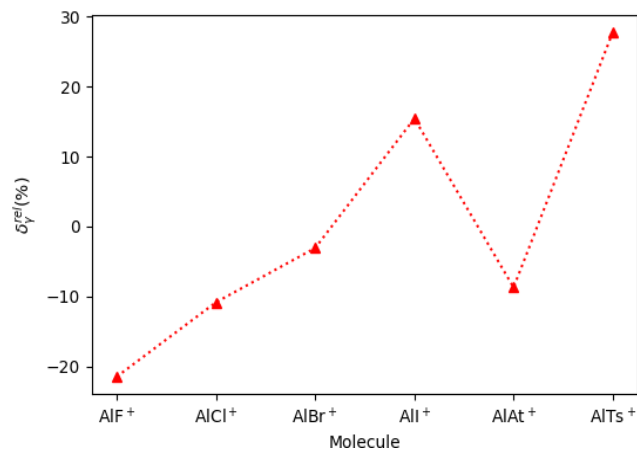


Figure 8. Figure showing the relative percentage changes in the  $\gamma$  values of the AlX<sup>+</sup> (X: F, Cl, Br, I, At and Ts) molecular systems due to the electron relativistic effects.

$\bar{\alpha}$  for AlBr<sup>+</sup> and AlAt<sup>+</sup>, while increasing it for the rest of the molecular ions. These effects result in an increase in the  $\gamma$  value for AlI<sup>+</sup> and AlTs<sup>+</sup>, while reducing it for the other molecular ions, with the most significant increase, at 28%, observed for the AlTs<sup>+</sup> molecular ion.

Similar to PDM, we have also checked the effect of diffuse functions on the components of static DP, utilizing singly augmented quadruple zeta basis sets. Table VI shows the outcomes for DPs using singly augmented basis sets. The augmentation of the basis sets does not notably alter the values of  $\bar{\alpha}$  and  $\gamma$  for

Table VI. Magnitude of permanent dipole moments (in Debye) and components of static dipole polarizability (in au) for  $\text{AlX}^+$  (X: F, Cl, Br, I, At and Ts) molecular systems at different levels of correlation using singly augmented quadruple zeta (s-aug-dyall.v4z) basis sets.

Molecule	Method	$\mu$	$\alpha_{\parallel}$	$\alpha_{\perp}$	$\bar{\alpha}$	$\gamma$
$\text{AlF}^+$	DHF	2.547	16.888	21.965	20.273	-5.077
	CCSD	2.297	19.168	21.982	21.044	-2.814
	CCSD(T)	2.219	19.795	22.100	21.332	-2.305
$\text{AlCl}^+$	DHF	0.740	38.611	31.287	33.728	7.324
	CCSD	0.349	43.075	31.415	35.302	11.660
	CCSD(T)	0.222	44.273	31.730	35.911	12.543
$\text{AlBr}^+$	DHF	0.483	51.815	36.609	41.678	15.206
	CCSD	0.031	57.397	36.711	43.606	20.686
	CCSD(T)	0.185	58.931	37.125	44.394	21.806
$\text{AlI}^+$	DHF	1.504	80.609	46.998	58.202	33.611
	CCSD	2.333	88.634	47.197	61.009	41.437
	CCSD(T)	2.512	98.517	48.095	64.902	50.422
$\text{AlAt}^+$	DHF	4.307	109.140	61.718	77.525	47.422
	CCSD	4.293	103.710	60.028	74.589	43.682
	CCSD(T)	4.309	106.039	55.382	72.268	50.657
$\text{AlTs}^+$	DHF	6.729	136.359	93.799	107.986	42.560
	CCSD	6.575	131.980	62.110	85.400	69.870
	CCSD(T)	6.687	133.300	60.291	84.627	73.009

molecular ions, except in the case of  $\text{AlF}^+$ , where there is a significant difference in the value of  $\gamma$  at CCSD(T) level of theory. Table IV shows that the  $\text{AlF}^+$  molecular ion exhibits a negative value of  $\gamma$  at the DHF and CCSD levels of theory; however, the value becomes positive at the CCSD(T) level of theory. Table VI illustrates that the value of  $\gamma$  adheres to the expected trend at different levels of correlation, emphasizing the importance of augmenting the basis sets for the  $\text{AlF}^+$  molecular ion. The negative values of  $\gamma$  have been reported in the literature for alkaline-earth monofluoride molecules in Ref. [43, 44].

We now discuss the possible sources of inaccuracies in our computations of static DP in the same way as that of PDM. We have found that increasing the virtual cut-off from  $12 E_h$  to  $25 E_h$  leads to a 1.1% change for  $\bar{\alpha}$  and a 0.4% change for  $\gamma$ , while including 49 active electrons changes  $\bar{\alpha}$  by 1% and  $\gamma$  by 1.9%. Furthermore, the addition of augmented functions to the basis sets changes  $\bar{\alpha}$  by 0.3% and  $\gamma$  by 0.6%. The error resulting from the missing triple excitations in the CCSD(T) method would be about 2.1% for  $\bar{\alpha}$  and 13% for  $\gamma$ . Hence, we anticipate an approximate 4.5% deviation for  $\bar{\alpha}$  and a 16% deviation for  $\gamma$  in our results.

#### IV. CONCLUSION

In summary, we have done fully relativistic calculations for the PDMs and the components of static DPs of singly charged aluminum monohalide ions at the DHF and CCSD(T) level of theory using a hierarchy of progressively larger Dyal basis sets. Our findings for the molecular PDMs for the ground electronic state of aluminum monohalides agree well with the existing values in the literature. We have reported the results of molecular DPs for the first time in the literature to the best of our knowledge. The roles of relativistic and correlation effects in determining the PDMs and static DPs have been studied extensively in this work. We found that correlation effects impact the precision of final PDM values, with  $\text{AlI}^+$  showing the maximum change at 62%, while the influence of relativity is particularly striking in superheavy  $\text{AlTs}^+$ , exhibiting the largest variation at 50%. We also observe that electron correlation tends to enhance  $\bar{\alpha}$  and  $\gamma$  for most molecules, whereas relativistic effects have varying impacts on these properties across different molecular ions. The effect of singly augmenting the basis sets on the molecular properties of the ground state is also investigated. Finally, we selected  $\text{AlAt}^+$  as our representative system to evaluate errors, and our findings indicate that various sources of errors contribute together by about 5.5% for the PDM, 4.5% for  $\bar{\alpha}$ , and 16% for  $\gamma$ . We anticipate

that our relativistic calculations, computed with large basis sets and large active space, would be beneficial for experimental spectroscopists interested in working with these molecular systems in the future.

## ACKNOWLEDGMENTS

We would like to thank the National Supercomputing Mission (NSM) for providing computing resources of ‘PARAM Ganga’ at the Indian Institute of Technology Roorkee, implemented by C-DAC and supported by the Ministry of Electronics and Information Technology (MeitY) and Department of Science and Technology (DST), Government of India. R.B. was supported by Polish National Science Centre Project No. 2021/41/B/ST2/00681. The research is also a part of the program of the National Laboratory FAMO in Toruń, Poland.

- 
- [1] L. D. Carr, D. DeMille, R. V. Krems, and J. Ye, Cold and ultracold molecules: science, technology and applications, *New J. Phys.* **11**, 055049 (2009).
- [2] C. Chin, V. V. Flambaum, and M. G. Kozlov, Ultracold molecules: new probes on the variation of fundamental constants, *New J. Phys.* **11**, 055048 (2009).
- [3] D. S. Jin and J. Ye, Introduction to ultracold molecules: New frontiers in quantum and chemical physics, *Chem. Rev.* **112**, 4801 (2012).
- [4] T. P. Softley, Cold and ultracold molecules in the twenties, *Proc. R. Soc. A* **479**, 20220806 (2023).
- [5] D. Mitra, K. H. Leung, and T. Zelevinsky, Quantum control of molecules for fundamental physics, *Phys. Rev. A* **105**, 040101 (2022).
- [6] M. T. Bell and T. P. Softley, Ultracold molecules and ultracold chemistry, *Mol. Phys.* **107**, 99 (2009).
- [7] S. L. Cornish, M. R. Tarbutt, and K. R. A. Hazzard, Quantum computation and quantum simulation with ultracold molecules, *Nat. Phys.* **20**, 730 (2024).
- [8] S. N. Tohme and M. Korek, Electronic structure calculation of the kyb molecule with dipole moments, polarizabilities, and ro-vibrational studies, *Comput. Theor. Chem.* **1078**, 65 (2016).
- [9] D. DeMille, Quantum computation with trapped polar molecules, *Phys. Rev. Lett.* **88**, 067901 (2002).
- [10] S. F. Yelin, K. Kirby, and R. Côté, Schemes for robust quantum computation with polar molecules, *Phys. Rev. A* **74**, 050301 (2006).
- [11] P. Rabl and P. Zoller, Molecular dipolar crystals as high-fidelity quantum memory for hybrid quantum computing, *Phys. Rev. A* **76**, 042308 (2007).
- [12] Z.-Y. Zhang, J.-M. Liu, Z. Hu, and Y. Wang, Implementation of three-qubit quantum computation with pendular states of polar molecules by optimal control, *J. Chem. Phys.* **152**, 044303 (2020).
- [13] A. D. Buckingham, Molecular quadrupole moments, *Q. Rev. Chem. Soc.* **13**, 183 (1959).
- [14] A. C. Vutha, W. C. Campbell, Y. V. Gurevich, N. R. Hutzler, M. Parsons, D. Patterson, E. Petrik, B. Spaun, J. M. Doyle, G. Gabrielse, and D. DeMille, Search for the electric dipole moment of the electron with thorium monoxide, *J. Phys. B: At. Mol. Opt. Phys.* **43**, 074007 (2010).
- [15] N. M. Fazil, V. S. Prasanna, K. V. P. Latha, M. Abe, and B. P. Das, Electron correlation trends in the permanent electric dipole moments of alkaline-earth-metal monohydrides, *Phys. Rev. A* **98**, 032511 (2018).
- [16] A. Sunaga, M. Abe, M. Hada, and B. P. Das, Merits of heavy-heavy diatomic molecules for electron electric-dipole-moment searches, *Phys. Rev. A* **99**, 062506 (2019).
- [17] V. S. Prasanna, A. Sunaga, M. Abe, M. Hada, N. Shitara, A. Sakurai, and B. P. Das, The role of relativistic many-body theory in electron electric dipole moment searches using cold molecules, *Atoms* **7**, 10.3390/atoms7020058 (2019).
- [18] T. Fleig, TaO<sup>+</sup> as a candidate molecular ion for searches of physics beyond the standard model, *Phys. Rev. A* **95**, 022504 (2017).
- [19] D.-W. Wang, M. D. Lukin, and E. Demler, Quantum fluids of self-assembled chains of polar molecules, *Phys. Rev. Lett.* **97**, 180413 (2006).
- [20] A. D. Buckingham, G. W. Series, E. R. Pike, and J. G. Powles, Polarizability and hyperpolarizability, *Phil. Trans. R. Soc. A* **293**, 239 (1979).
- [21] N. F. Lane, The theory of electron-molecule collisions, *Rev. Mod. Phys.* **52**, 29 (1980).
- [22] B. I. Loukhovitski and A. S. Sharipov, Molecular collision diameters and electronic polarizabilities: Inherent relationship and fast evaluation, *J. Phys. Chem. A* **125**, 5117 (2021).
- [23] C. N. Banwell, *Fundamentals of molecular spectroscopy*, European chemistry series (McGraw-Hill, 1972) Chap. 3, 4.
- [24] S.-Y. Kang, F.-G. Kuang, G. Jiang, D.-B. Li, Y. Luo, P. Feng-Hui, W. Li-Ping, W.-Q. Hu, and Y.-C. Shao, *Ab initio* study of laser cooling of AlF<sup>+</sup> and AlCl<sup>+</sup> molecular ions, *J. Phys. B: At. Mol. Opt. Phys.* **50**, 105103 (2017).

- [25] R. Klein and P. Rosmus, Ab initio calculations of infrared transition probabilities in the electronic ground states of AlF and AlF<sup>+</sup>, *Theor. Chim. Acta* **66**, 21 (1984).
- [26] T. Glenewinkel-Meyer, B. Müller, C. Ottinger, P. Rosmus, P. J. Knowles, and H. Werner, Ab initio calculations on the four lowest electronic states of AlF<sup>+</sup> and AlCl<sup>+</sup>, *J. Chem. Phys.* **95**, 5133 (1991).
- [27] R. Bala, V. S. Prasanna, and B. P. Das, Relativistic calculations of molecular electric dipole moments of singly charged aluminium monohalides, *J. Phys. B: At. Mol. Opt. Phys.* **56**, 125101 (2023).
- [28] K. G. Dyall, Relativistic quadruple-zeta and revised triple-zeta and double-zeta basis sets for the 4p, 5p, and 6p elements, *Theor. Chem. Acc.* **115**, 441 (2006).
- [29] K. G. Dyall, Relativistic double-zeta, triple-zeta, and quadruple-zeta basis sets for the light elements H-Ar, *Theor. Chem. Acc.* **135**, 128 (2016).
- [30] I. Shavitt and R. J. Bartlett, *Many-Body Methods in Chemistry and Physics: MBPT and Coupled-Cluster Theory*, Cambridge Molecular Science (Cambridge University Press, 2009) Chap. 9.
- [31] R. Mitra, V. S. Prasanna, and B. K. Sahoo, Comparative analysis of nonrelativistic and relativistic calculations of electric dipole moments and polarizabilities of heteronuclear alkali-metal dimers, *Phys. Rev. A* **101**, 012511 (2020).
- [32] R. Bast, A. S. P. Gomes, T. Saue, L. Visscher, H. J. A. Jensen, with contributions from I. A. Aucar, V. Bakken, C. Chibueze, J. Creutzberg, K. G. Dyall, S. Dubillard, U. Ekström, E. Eliav, T. Enevoldsen, E. Faßhauer, T. Fleig, O. Fossgaard, L. Halbert, E. D. Hedegård, T. Helgaker, B. Helmich-Paris, J. Henriksson, M. van Horn, M. Iliaš, C. R. Jacob, S. Knecht, S. Komorovský, O. Kullie, J. K. Lærdahl, C. V. Larsen, Y. S. Lee, N. H. List, H. S. Nataraj, M. K. Nayak, P. Norman, A. Nyvang, G. Olejniczak, J. Olsen, J. M. H. Olsen, A. Papadopoulos, Y. C. Park, J. K. Pedersen, M. Pernpointner, J. V. Pototschnig, R. D. Remigio, M. Repisky, K. Ruud, P. Sałek, B. Schimmelpfennig, B. Senjean, A. Shee, J. Sikkema, A. Sunaga, A. J. Thorvaldsen, J. Thyssen, J. van Stralen, M. L. Vidal, S. Villaume, O. Visser, T. Winther, S. Yamamoto, and X. Yuan, *DIRAC, a relativistic ab initio electronic structure program, Release DIRAC23*, (2023 (<http://www.diracprogram.org>)), available at <https://doi.org/10.5281/zenodo.7670749>.
- [33] K. G. Dyall and K. Faegri, *Introduction to Relativistic Quantum Chemistry* (Oxford University Press, 2007) Chap. 11.
- [34] L. Visscher, Approximate molecular relativistic dirac-coulomb calculations using a simple coulombic correction, *Theor. Chem. Acc.* **98**, 68 (1997).
- [35] K. A. Peterson, D. E. Woon, and J. Dunning, Thom H., Benchmark calculations with correlated molecular wave functions. IV. The classical barrier height of the H+H<sub>2</sub>→H<sub>2</sub>+H reaction, *J. Chem. Phys.* **100**, 7410 (1994).
- [36] D. Feller and J. A. Sordo, A ccsdt study of the effects of higher order correlation on spectroscopic constants. I. first row diatomic hydrides, *J. Chem. Phys.* **112**, 5604 (2000).
- [37] R. Bala, H. Nataraj, M. Abe, and M. Kajita, Accurate ab initio calculations of spectroscopic constants and properties of BeLi<sup>+</sup>, *J. Mol. Spectrosc.* **349**, 1 (2018).
- [38] R. J. Bartlett and M. Musiał, Coupled-cluster theory in quantum chemistry, *Rev. Mod. Phys.* **79**, 291 (2007).
- [39] B. K. Sahoo and P. Kumar, Relativistic coupled-cluster-theory analysis of unusually large correlation effects in the determination of *g<sub>j</sub>* factors in Ca<sup>+</sup>, *Phys. Rev. A* **96**, 012511 (2017).
- [40] R. de Berrêdo, F. Jorge, S. S. Jorge, and R. Centoducatte, An augmented gaussian basis set for calculations of molecular polarizabilities on platinum compounds, *Comput. Theor. Chem.* **965**, 236 (2011).
- [41] R. Maitra, Y. Akinaga, and T. Nakajima, A coupled cluster theory with iterative inclusion of triple excitations and associated equation of motion formulation for excitation energy and ionization potential, *J. Chem. Phys.* **147**, 074103 (2017).
- [42] P. J. Dagdigian, J. Graff, and L. Wharton, Stark Effect of NaLi X <sup>1</sup>Σ<sup>+</sup>, *J. Chem. Phys.* **55**, 4980 (1971).
- [43] S. L. Davis, Model polarizabilities and multipoles for ionic compounds. Alkaline-earth monohalides, *J. Chem. Phys.* **89**, 1656 (1988).
- [44] R. Bala, H. S. Nataraj, and M. K. Nayak, Ab initio calculations of permanent dipole moments and dipole polarizabilities of alkaline-earth monofluorides, *J. Phys. B: At. Mol. Opt. Phys.* **52**, 085101 (2019).